

Measurement of the t Distribution in Diffractive Photoproduction at HERA

The ZEUS Collaboration

Abstract

Photon diffractive dissociation, $\gamma p \rightarrow Xp$, has been studied at HERA with the ZEUS detector using ep interactions where the virtuality Q^2 of the exchanged photon is smaller than 0.02 GeV^2 . The squared four-momentum t exchanged at the proton vertex was determined in the range $0.073 < |t| < 0.40 \text{ GeV}^2$ by measuring the scattered proton in the ZEUS Leading Proton Spectrometer. In the photon-proton centre-of-mass energy interval $176 < W < 225 \text{ GeV}$ and for masses of the dissociated photon system $4 < M_X < 32 \text{ GeV}$, the t distribution has an exponential shape, $dN/d|t| \propto \exp(-b|t|)$, with a slope parameter $b = 6.8 \pm 0.9$ (stat.) $^{+1.2}_{-1.1}$ (syst.) GeV^{-2} .

The ZEUS Collaboration

J. Breitweg, M. Derrick, D. Krakauer, S. Magill, D. Mikunas, B. Musgrave, J. Repond, R. Stanek, R.L. Talaga, R. Yoshida, H. Zhang

Argonne National Laboratory, Argonne, IL, USA ^p

M.C.K. Mattingly

Andrews University, Berrien Springs, MI, USA

F. Anselmo, P. Antonioli, G. Bari, M. Basile, L. Bellagamba, D. Boscherini, A. Bruni, G. Bruni, G. Cara Romeo, G. Castellini¹, M. Chiarini, L. Cifarelli², F. Cindolo, A. Contin, M. Corradi, S. De Pasquale, I. Gialas³, P. Giusti, G. Iacobucci, G. Laurenti, G. Levi, A. Margotti, T. Massam, R. Nania, C. Nemoz⁴, F. Palmonari, A. Pesci, A. Polini, F. Ricci, G. Sartorelli, Y. Zamora Garcia⁵, A. Zichichi

University and INFN Bologna, Bologna, Italy ^f

C. Amelung, A. Bornheim, I. Brock, K. Coböken, J. Crittenden, R. Deffner, M. Eckert, M. Grothe, H. Hartmann, K. Heinloth, L. Heinz, E. Hilger, H.-P. Jakob, U.F. Katz, R. Kerger, E. Paul, M. Pfeiffer, Ch. Rembser⁶, J. Stamm, R. Wedemeyer⁷, H. Wieber

Physikalisches Institut der Universität Bonn, Bonn, Germany ^c

D.S. Bailey, S. Campbell-Robson, W.N. Cottingham, B. Foster, R. Hall-Wilton, M.E. Hayes, G.P. Heath, H.F. Heath, J.D. McFall, D. Piccioni, D.G. Roff, R.J. Tapper

H.H. Wills Physics Laboratory, University of Bristol, Bristol, U.K. ^o

M. Arneodo⁸, R. Ayad, M. Capua, A. Garfagnini, L. Iannotti, M. Schioppa, G. Susinno

Calabria University, Physics Dept. and INFN, Cosenza, Italy ^f

J.Y. Kim, J.H. Lee, I.T. Lim, M.Y. Pac⁹

Chonnam National University, Kwangju, Korea ^h

A. Caldwell¹⁰, N. Cartiglia, Z. Jing, W. Liu, B. Mellado, J.A. Parsons, S. Ritz¹¹, S. Sampson, F. Sciulli, P.B. Straub, Q. Zhu

Columbia University, Nevis Labs., Irvington on Hudson, N.Y., USA ^q

P. Borzemski, J. Chwastowski, A. Eskreys, J. Figiel, K. Klimek, M.B. Przybycień, L. Zawiejski

Inst. of Nuclear Physics, Cracow, Poland ^j

L. Adamczyk¹², B. Bednarek, M. Bukowy, A. Czermak, K. Jeleń, D. Kisielewska, T. Kowalski, M. Przybycień, E. Rulikowska-Zarebska, L. Suszycki, J. Zajac

Faculty of Physics and Nuclear Techniques, Academy of Mining and Metallurgy, Cracow, Poland ^j

Z. Duliński, A. Kotański

Jagellonian Univ., Dept. of Physics, Cracow, Poland ^k

G. Abbiendi¹³, L.A.T. Bauerdick, U. Behrens, H. Beier, J.K. Bienlein, G. Cases¹⁴, O. Deppe, K. Desler, G. Drews, U. Fricke, D.J. Gilkinson, C. Glasman, P. Göttlicher, T. Haas, W. Hain, D. Hasell, K.F. Johnson¹⁵, M. Kasemann, W. Koch, U. Kötz, H. Kowalski, J. Labs, L. Lindemann, B. Löhr, M. Löwe¹⁶, O. Mańczak, J. Milewski, T. Monteiro¹⁷, J.S.T. Ng¹⁸, D. Notz, K. Ohrenberg¹⁹, I.H. Park²⁰, A. Pellegrino, F. Pelucchi, K. Piotrkowski, M. Roco²¹, M. Rohde, J. Roldán, J.J. Ryan, A.A. Savin, U. Schneekloth, O. Schwarzer, F. Selonke, B. Surrow, E. Tassi, T. Voß²², D. Westphal, G. Wolf, U. Wollmer²³, C. Youngman, A.F. Żarnecki, W. Zeuner
Deutsches Elektronen-Synchrotron DESY, Hamburg, Germany

B.D. Burow, H.J. Grabosch, A. Meyer, S. Schlenstedt
DESY-IfH Zeuthen, Zeuthen, Germany

G. Barbagli, E. Gallo, P. Pelfer
University and INFN, Florence, Italy^f

G. Anzivino²⁴, G. Maccarrone, L. Votano
INFN, Laboratori Nazionali di Frascati, Frascati, Italy^f

A. Bamberger, S. Eisenhardt, P. Markun, T. Trefzger²⁵, S. Wölffe
Fakultät für Physik der Universität Freiburg i.Br., Freiburg i.Br., Germany^c

J.T. Bromley, N.H. Brook, P.J. Bussey, A.T. Doyle, N. Macdonald, D.H. Saxon, L.E. Sinclair, E. Strickland, R. Waugh
Dept. of Physics and Astronomy, University of Glasgow, Glasgow, U.K.^o

I. Bohnet, N. Gendner, U. Holm, A. Meyer-Larsen, H. Salehi, K. Wick
Hamburg University, I. Institute of Exp. Physics, Hamburg, Germany^c

L.K. Gladilin²⁶, D. Horstmann, D. Kçira²⁷, R. Klanner, E. Lohrmann, G. Poelz, W. Schott²⁸, F. Zetsche
Hamburg University, II. Institute of Exp. Physics, Hamburg, Germany^c

T.C. Bacon, I. Butterworth, J.E. Cole, G. Howell, B.H.Y. Hung, L. Lamberti²⁹, K.R. Long, D.B. Miller, N. Pavel, A. Prinias³⁰, J.K. Sedgbeer, D. Sideris, R. Walker
Imperial College London, High Energy Nuclear Physics Group, London, U.K.^o

U. Mallik, S.M. Wang, J.T. Wu
University of Iowa, Physics and Astronomy Dept., Iowa City, USA^p

P. Cloth, D. Filges
Forschungszentrum Jülich, Institut für Kernphysik, Jülich, Germany

J.I. Fleck⁶, T. Ishii, M. Kuze, I. Suzuki³¹, K. Tokushuku, S. Yamada, K. Yamauchi, Y. Yamazaki³²
Institute of Particle and Nuclear Studies, KEK, Tsukuba, Japan^g

S.J. Hong, S.B. Lee, S.W. Nam³³, S.K. Park
Korea University, Seoul, Korea^h

F. Barreiro, J.P. Fernández, G. García, R. Graciani, J.M. Hernández, L. Hervás⁶, L. Labarga, M. Martínez, J. del Peso, J. Puga, J. Terrón, J.F. de Trocóniz
Univer. Autónoma Madrid, Depto de Física Teórica, Madrid, Spainⁿ

F. Corriveau, D.S. Hanna, J. Hartmann, L.W. Hung, W.N. Murray, A. Ochs, M. Riveline, D.G. Stairs, M. St-Laurent, R. Ullmann

McGill University, Dept. of Physics, Montréal, Québec, Canada^{a, b}

T. Tsurugai

Meiji Gakuin University, Faculty of General Education, Yokohama, Japan

V. Bashkirov, B.A. Dolgoshein, A. Stifutkin

Moscow Engineering Physics Institute, Moscow, Russia^l

G.L. Bashindzhagyan, P.F. Ermolov, Yu.A. Golubkov, L.A. Khein, N.A. Korotkova, I.A. Korzhavina, V.A. Kuzmin, O.Yu. Lukina, A.S. Proskuryakov, L.M. Shcheglova³⁴, A.N. Solomin³⁴, S.A. Zotkin

Moscow State University, Institute of Nuclear Physics, Moscow, Russia^m

C. Bokel, M. Botje, N. Brümmer, F. Chlebana²¹, J. Engelen, E. Koffeman, P. Kooijman, A. van Sighem, H. Tiecke, N. Tuning, W. Verkerke, J. Vosseveld, M. Vreeswijk⁶, L. Wiggers, E. de Wolf

*NIKHEF and University of Amsterdam, Amsterdam, Netherlands*ⁱ

D. Acosta, B. Bylsma, L.S. Durkin, J. Gilmore, C.M. Ginsburg, C.L. Kim, T.Y. Ling, P. Nylander, T.A. Romanowski³⁵

Ohio State University, Physics Department, Columbus, Ohio, USA^p

H.E. Blaikley, R.J. Cashmore, A.M. Cooper-Sarkar, R.C.E. Devenish, J.K. Edmonds, J. Große-Knetter³⁶, N. Harnew, C. Nath, V.A. Noyes³⁷, A. Quadt, O. Ruske, J.R. Tickner³⁰, H. Uijterwaal, R. Walczak, D.S. Waters

Department of Physics, University of Oxford, Oxford, U.K.^o

A. Bertolin, R. Brugnera, R. Carlin, F. Dal Corso, U. Dosselli, S. Limentani, M. Morandin, M. Posocco, L. Stanco, R. Stroili, C. Voci

Dipartimento di Fisica dell' Università and INFN, Padova, Italy^f

J. Bulmahn, B.Y. Oh, J.R. Okrasinski, W.S. Toothacker, J.J. Whitmore

Pennsylvania State University, Dept. of Physics, University Park, PA, USA^q

Y. Iga

Polytechnic University, Sagamihara, Japan^g

G. D'Agostini, G. Marini, A. Nigro, M. Raso

Dipartimento di Fisica, Univ. 'La Sapienza' and INFN, Rome, Italy^f

J.C. Hart, N.A. McCubbin, T.P. Shah

Rutherford Appleton Laboratory, Chilton, Didcot, Oxon, U.K.^o

D. Epperson, C. Heusch, J.T. Rahn, H.F.-W. Sadrozinski, A. Seiden, R. Wichmann, D.C. Williams

University of California, Santa Cruz, CA, USA^p

H. Abramowicz³⁸, G. Briskin, S. Dagan³⁸, S. Kananov³⁸, A. Levy³⁸

Raymond and Beverly Sackler Faculty of Exact Sciences, School of Physics, Tel-Aviv University, Tel-Aviv, Israel^e

T. Abe, T. Fusayasu, M. Inuzuka, K. Nagano, K. Umemori, T. Yamashita
Department of Physics, University of Tokyo, Tokyo, Japan^g

R. Hamatsu, T. Hirose, K. Homma³⁹, S. Kitamura⁴⁰, T. Matsushita
Tokyo Metropolitan University, Dept. of Physics, Tokyo, Japan^g

R. Cirio, M. Costa, M.I. Ferrero, S. Maselli, V. Monaco, C. Peroni, M.C. Petrucci, M. Ruspa,
R. Sacchi, A. Solano, A. Staiano
Università di Torino, Dipartimento di Fisica Sperimentale and INFN, Torino, Italy^f

M. Dardo
II Faculty of Sciences, Torino University and INFN - Alessandria, Italy^f

D.C. Bailey, C.-P. Fagerstroem, R. Galea, G.F. Hartner, K.K. Joo, G.M. Levman, J.F. Martin,
R.S. Orr, S. Polenz, A. Sabetfakhri, D. Simmons, R.J. Teuscher⁶
University of Toronto, Dept. of Physics, Toronto, Ont., Canada^a

J.M. Butterworth, C.D. Catterall, T.W. Jones, J.B. Lane, R.L. Saunders, M.R. Sutton, M. Wing
University College London, Physics and Astronomy Dept., London, U.K.^o

J. Ciborowski, G. Grzelak⁴¹, M. Kasprzak, K. Muchorowski⁴², R.J. Nowak, J.M. Pawlak,
R. Pawlak, T. Tymieniecka, A.K. Wróblewski, J.A. Zakrzewski
Warsaw University, Institute of Experimental Physics, Warsaw, Poland^j

M. Adamus
Institute for Nuclear Studies, Warsaw, Poland^j

C. Coldewey, Y. Eisenberg³⁸, D. Hochman, U. Karshon³⁸
Weizmann Institute, Department of Particle Physics, Rehovot, Israel^d

W.F. Badgett, D. Chapin, R. Cross, S. Dasu, C. Foudas, R.J. Loveless, S. Mattingly, D.D. Reeder,
W.H. Smith, A. Vaiciulis, M. Wodarczyk
University of Wisconsin, Dept. of Physics, Madison, WI, USA^p

A. Deshpande, S. Dhawan, V.W. Hughes
Yale University, Department of Physics, New Haven, CT, USA^p

S. Bhadra, W.R. Frisken, M. Khakzad, W.B. Schmidke
York University, Dept. of Physics, North York, Ont., Canada^a

¹ also at IROE Florence, Italy
² now at Univ. of Salerno and INFN Napoli, Italy
³ now at Univ. of Crete, Greece
⁴ now at E.S.R.F., BP220, F-38043 Grenoble, France
⁵ supported by Worldlab, Lausanne, Switzerland
⁶ now at CERN
⁷ retired
⁸ also at University of Torino and Alexander von Humboldt Fellow at DESY
⁹ now at Dongshin University, Naju, Korea
¹⁰ also at DESY
¹¹ Alfred P. Sloan Foundation Fellow
¹² supported by the Polish State Committee for Scientific Research, grant No. 2P03B14912
¹³ supported by an EC fellowship number ERBFMBICT 950172
¹⁴ now at SAP A.G., Walldorf
¹⁵ visitor from Florida State University
¹⁶ now at ALCATEL Mobile Communication GmbH, Stuttgart
¹⁷ supported by European Community Program PRAXIS XXI
¹⁸ now at DESY-Group FDET
¹⁹ now at DESY Computer Center
²⁰ visitor from Kyungpook National University, Taegu, Korea, partially supported by DESY
²¹ now at Fermi National Accelerator Laboratory (FNAL), Batavia, IL, USA
²² now at NORCOM Infosystems, Hamburg
²³ now at Oxford University, supported by DAAD fellowship HSP II-AUFE III
²⁴ now at University of Perugia, I-06100 Perugia, Italy
²⁵ now at ATLAS Collaboration, Univ. of Munich
²⁶ on leave from MSU, supported by the GIF, contract I-0444-176.07/95
²⁷ supported by DAAD, Bonn
²⁸ now a self-employed consultant
²⁹ supported by an EC fellowship
³⁰ PPARC Post-doctoral Fellow
³¹ now at Osaka Univ., Osaka, Japan
³² supported by JSPS Postdoctoral Fellowships for Research Abroad
³³ now at Wayne State University, Detroit
³⁴ partially supported by the Foundation for German-Russian Collaboration DFG-RFBR
(grant no. 436 RUS 113/248/3 and no. 436 RUS 113/248/2)
³⁵ now at Department of Energy, Washington
³⁶ supported by the Feodor Lynen Program of the Alexander von Humboldt foundation
³⁷ Glasstone Fellow
³⁸ supported by a MINERVA Fellowship
³⁹ now at ICEPP, Univ. of Tokyo, Tokyo, Japan
⁴⁰ present address: Tokyo Metropolitan College of Allied Medical Sciences, Tokyo 116, Japan
⁴¹ supported by the Polish State Committee for Scientific Research, grant No. 2P03B09308
⁴² supported by the Polish State Committee for Scientific Research, grant No. 2P03B09208

- a* supported by the Natural Sciences and Engineering Research Council of Canada (NSERC)
- b* supported by the FCAR of Québec, Canada
- c* supported by the German Federal Ministry for Education and Science, Research and Technology (BMBF), under contract numbers 057BN19P, 057FR19P, 057HH19P, 057HH29P, 057SI75I
- d* supported by the MINERVA Gesellschaft für Forschung GmbH, the German Israeli Foundation, and the U.S.-Israel Binational Science Foundation
- e* supported by the German Israeli Foundation, and by the Israel Science Foundation
- f* supported by the Italian National Institute for Nuclear Physics (INFN)
- g* supported by the Japanese Ministry of Education, Science and Culture (the Monbusho) and its grants for Scientific Research
- h* supported by the Korean Ministry of Education and Korea Science and Engineering Foundation
- i* supported by the Netherlands Foundation for Research on Matter (FOM)
- j* supported by the Polish State Committee for Scientific Research, grant No. 115/E-343/SPUB/P03/002/97, 2P03B10512, 2P03B10612, 2P03B14212, 2P03B10412
- k* supported by the Polish State Committee for Scientific Research (grant No. 2P03B08308) and Foundation for Polish-German Collaboration
- l* partially supported by the German Federal Ministry for Education and Science, Research and Technology (BMBF)
- m* supported by the Fund for Fundamental Research of Russian Ministry for Science and Education and by the German Federal Ministry for Education and Science, Research and Technology (BMBF)
- n* supported by the Spanish Ministry of Education and Science through funds provided by CICYT
- o* supported by the Particle Physics and Astronomy Research Council
- p* supported by the US Department of Energy
- q* supported by the US National Science Foundation

1 Introduction

The reaction $\gamma p \rightarrow Xp$, in which the photon diffractively dissociates into an hadronic state X with mass M_X , has been investigated with real photons at a photon-proton centre-of-mass energy W of about 14 GeV [1]. Recently it has also been studied at HERA using the process $ep \rightarrow eXp$ for photon virtualities $Q^2 < 0.02 \text{ GeV}^2$ and $W \approx 200 \text{ GeV}$ [2, 3]. The comparison of the fixed target data and the HERA data indicates that the dissociation of real photons has similar characteristics to the dissociation of hadrons, as expected in the framework of Vector Meson Dominance (VMD) [4, 5]. In this model, the photon is assumed to fluctuate into a virtual vector meson prior to the interaction with the proton. The interaction can be described by Regge phenomenology [6] and, at high energy, is dominated by the exchange of an object with the quantum numbers of the vacuum, referred to as the pomeron. An exponential fall of the differential cross section $d\sigma/d|t| \propto \exp(-b|t|)$, at small values of $|t|$, is a typical feature of diffraction; here t is the square of the four-momentum transfer at the proton vertex. Regge theory also predicts that the diffractive peak shrinks as W increases according to $b = b_0 + 2\alpha' \ln(W^2/M_X^2)$, where b_0 and α' are constants [6, 7].

The studies of diffractive real photon dissociation at HERA have so far focussed on the shape of the M_X spectrum [2, 3]. The t distribution for the reaction $\gamma p \rightarrow Xp$ has been measured only by the fixed target experiment [1], which found that in the range $1.4 < M_X < 3 \text{ GeV}$ and for $0.02 < |t| < 0.1 \text{ GeV}^2$ the t dependence is exponential with a t -slope $b \approx 5 \text{ GeV}^{-2}$. At HERA, measurements of the t distribution have been performed for the diffractive dissociation of virtual photons in the range $5 < Q^2 < 20 \text{ GeV}^2$ [8], and for elastic vector meson production, $\gamma p \rightarrow Vp$, both with real and with virtual photons [9-18]. In all cases the distribution has an approximately exponential shape. The t -slope is $b = 7.2 \pm 1.1 \text{ (stat.) } {}^{+0.7}_{-0.9} \text{ (syst.) GeV}^{-2}$ for the diffractive dissociation of virtual photons at $\langle Q^2 \rangle = 8 \text{ GeV}^2$. For elastic ρ^0 production b depends only weakly on W but varies from approximately 10 GeV^{-2} for $Q^2 \approx 0$ [9-11] to approximately $5\text{-}7 \text{ GeV}^{-2}$ for $\langle Q^2 \rangle = 10 \text{ GeV}^2$ [12, 13]. It is therefore interesting to extend these measurements to diffractive real photon dissociation.

In this paper we report the first determination at HERA of the t distribution for the process $\gamma p \rightarrow Xp$, where γ is a photon with $Q^2 < 0.02 \text{ GeV}^2$. The present measurement is based on a sample of photoproduction events collected using the reaction $ep \rightarrow eXp$ at $W \approx 200 \text{ GeV}$ [3]. The sample was defined by the requirement that the scattered positron be measured in a calorimeter close to the outgoing positron beam line and a final state proton carrying at least 97% of the incoming proton momentum be detected in the ZEUS Leading Proton Spectrometer (LPS) [11]. The LPS was also used to measure the transverse momentum of the proton, from which t was calculated. This is a technique similar to that used to measure the t distribution in the photoproduction of ρ^0 mesons, $\gamma p \rightarrow \rho^0 p$ [11], and for the diffractive dissociation of virtual photons, $\gamma^* p \rightarrow Xp$ [8].

2 Experimental set-up

2.1 HERA

The data presented here were collected in 1994 at HERA which operated with 820 GeV protons and 27.5 GeV positrons. The proton and positron beams each contained 153 colliding bunches,

together with 17 additional unpaired proton and 15 unpaired positron bunches. These additional bunches were used for background studies. The integrated luminosity for the present study, which required the LPS to be in operation, is 0.9 pb^{-1} .

2.2 The ZEUS detector

A detailed description of the ZEUS detector can be found elsewhere [19, 20]. A brief outline of the components which are most relevant for this analysis is given below. Throughout this paper the standard ZEUS coordinate system is used, which has the origin at the nominal interaction point, the Z axis pointing in the proton beam direction, hereafter referred to as “forward”, the X axis pointing horizontally towards the centre of HERA and the Y axis pointing upwards. The polar angle θ is defined with respect to the Z direction.

Charged particles are measured by the inner tracking detectors which operate in a magnetic field of 1.43 T provided by a thin superconducting solenoid. Immediately surrounding the beam-pipe is the vertex detector (VXD), a drift chamber which consists of 120 radial cells, each with 12 sense wires [21]. It is surrounded in turn by the central tracking detector (CTD), which consists of 72 cylindrical drift chamber layers, organized into 9 superlayers covering the polar angle region $15^\circ < \theta < 164^\circ$ [22].

For the energy measurement the high resolution depleted-uranium scintillator calorimeter (CAL) is used [23]. It is divided into three parts, forward (FCAL) covering the pseudorapidity¹ region $4.3 > \eta > 1.1$, barrel (BCAL) covering the central region $1.1 > \eta > -0.75$ and rear (RCAL) covering the backward region $-0.75 > \eta > -3.8$. Holes of $20 \times 20 \text{ cm}^2$ in the centre of FCAL and RCAL accommodate the HERA beam-pipe. Each of the calorimeter parts is subdivided into towers, which in turn are segmented longitudinally into electromagnetic (EMC) and hadronic (HAC) sections. These sections are further subdivided into cells, which are read out by two photomultiplier tubes. Under test beam conditions, the energy resolution of the calorimeter was measured to be $\sigma_E/E = 0.18/\sqrt{E(\text{GeV})}$ for electrons and $\sigma_E/E = 0.35/\sqrt{E(\text{GeV})}$ for hadrons. The calorimeter noise, dominated by the uranium radioactivity, is in the range 15-19 MeV for an EMC cell and 24-30 MeV for a HAC cell.

The luminosity is determined from the rate of the Bethe-Heitler process, $ep \rightarrow e\gamma p$, where the photon is measured with a lead-scintillator sandwich calorimeter (LUMI- γ) located at $Z = -107 \text{ m}$ in the HERA tunnel downstream of the interaction point in the direction of the outgoing positrons [24]. A similar calorimeter (LUMI- e) at $Z = -35 \text{ m}$ detects positrons scattered at very small angles. In this analysis, the LUMI- e was used to tag photoproduction events with positrons scattered at angles up to about 5 mrad and to measure the scattered positron energy, E'_e . The LUMI- e covers the range $7 < E'_e < 21 \text{ GeV}$. The energy resolution of both calorimeters is $\sigma_E/E = 0.18/\sqrt{E(\text{GeV})}$.

The Leading Proton Spectrometer (LPS) [11] detects charged particles scattered at small angles and carrying a substantial fraction, x_L , of the incoming proton momentum; these particles remain in the beam-pipe and their trajectory is measured by a system of silicon micro-strip detectors very close (typically a few mm) to the proton beam. The detectors are grouped in six stations, S1 to S6, placed along the beam line in the direction of the outgoing protons, at 23.8 m,

¹The pseudorapidity η is defined as $\eta = -\ln(\tan(\theta/2))$.

40.3 m, 44.5 m, 63.0 m, 81.2 m and 90.0 m from the interaction point. The track deflections induced by the magnets in the proton beam line allow a momentum analysis of the scattered proton. For the present measurements, only the stations S4, S5 and S6 were used. With this configuration, for x_L close to unity, resolutions of 0.4% on the longitudinal momentum and 5 MeV on the transverse momentum have been achieved. The effective transverse momentum resolution is, however, dominated by the intrinsic transverse momentum spread of the proton beam at the interaction point which is ≈ 40 MeV in the horizontal plane and ≈ 90 MeV in the vertical plane. For x_L close to unity, the LPS covers the range $0.25 \lesssim p_T \lesssim 0.65$ GeV, where p_T is the transverse momentum of the proton with respect to the incoming beam direction. As discussed previously [11], the incoming beam direction and the beam position with respect to each station are determined using the reaction $ep \rightarrow e\rho^0p$ at $Q^2 \approx 0$. Protons with $p_T < 0.2$ GeV and $x_L \approx 1$ are too close to the beam to be measured. For the events considered here the geometric acceptance of the LPS is approximately 6%.

3 Data selection and background subtraction

3.1 Trigger

ZEUS uses a three-level trigger system [19, 20]. At the first-level a coincidence between signals in the LUMI- e and in the RCAL was required. An energy deposit greater than 5 GeV was required in the LUMI- e . In the RCAL the deposit had to be larger than 464 MeV (excluding the towers immediately adjacent to the beam-pipe) or 1250 MeV (including those towers). The angular acceptance of the LUMI- e limits the Q^2 range to the region $Q^2 < 0.02$ GeV². The small RCAL threshold essentially selects all photoproduction events. The second and third trigger levels were mainly used to reject beam related background. Parts of the data stream were prescaled [3, 25] in order to reduce the high event rate resulting from the large photoproduction cross section.

3.2 Reconstruction of variables

The photon-proton centre-of-mass energy squared, $W^2 = (q + p)^2$, where q and p are the virtual photon and the proton four-momenta, respectively, was determined by $W^2 \approx ys$, with $y \approx E_\gamma/E_e = (E_e - E'_e)/E_e$ and s the squared centre-of-mass energy of the positron-proton system; here E_γ is the energy of the exchanged photon and E_e denotes the energy of the incoming positron. The W resolution is 7 GeV at $W = 176$ GeV and improves to 4.5 GeV at $W = 225$ GeV.

The mass M_X of the dissociated photon system was reconstructed [3] by combining the information from the LUMI- e and the CAL:

$$M_X = \sqrt{E^2 - P^2} \approx \sqrt{(E - P_Z) \cdot (E + P_Z)} = \sqrt{2E_\gamma \cdot (E + P_Z)}, \quad (1)$$

where E is the energy of the hadronic system observed in the CAL; the total momentum of the hadronic system, P , approximately equals the longitudinal component, P_Z , as the transverse

component generally is small in the case of photoproduction events. The following formula was used for the mass reconstruction:

$$M_{X\ rec} = a_1 \cdot \sqrt{2E_\gamma \cdot \left(\sum_{cond} E_i + \sum_{cond} E_i \cos \theta_i \right)} + a_2. \quad (2)$$

The quantities E_i and θ_i denote the energy and the polar angle of CAL condensates, defined as groups of adjacent cells with total energy of at least 100 MeV, if all the cells belong to the EMC, or 200 MeV otherwise. These cuts reduce the effect of noise on the mass reconstruction. They were applied in addition to a noise suppression algorithm which discarded all EMC (HAC) cells with energy below 60 MeV (110 MeV); for isolated cells the thresholds were increased to 80 MeV (120 MeV). The coefficients a_1 and a_2 correct for the effects of energy loss in the inactive material in front of the CAL and of energy deposits below the threshold. Their values, $a_1 = 1.14$ and $a_2 = 1.2$ GeV, were taken from [3]. The masses in the range $4 < M_X < 40$ GeV are reconstructed with a resolution $\sigma_{M_X}/M_X \approx 0.8/\sqrt{M_X(\text{GeV})}$ and an offset smaller than 0.5 GeV [3].

The variable $t = (p - p')^2$, where p and p' are the incoming and the scattered proton four-momenta, respectively, can be evaluated as $t \approx -(p_T^2/x_L)[1 + (M_p^2/p_T^2)(1 - x_L)^2]$. Both p_T and x_L were measured with the LPS. For the data considered here, which have x_L close to unity, the approximation $t \approx -p_T^2/x_L$ was used. Since, as mentioned earlier, the incoming proton beam has an intrinsic transverse momentum spread of $\sigma_{p_X} \approx 40$ MeV and $\sigma_{p_Y} \approx 90$ MeV, which is much larger than the LPS resolution in transverse momentum, the measured value of t is given by the convolution of the true t distribution and the effect of the beam spread. Because of this we make a distinction between the true value of t and the measured value, $t_{apparent} = -p_T^2/x_L$.

3.3 Offline selection

To select the final sample, the following conditions were imposed on the reconstructed data:

- A scattered positron in the LUMI- e with energy in the range $12 < E'_e < 18$ GeV, corresponding to $176 < W < 225$ GeV.
- An interaction vertex reconstructed by the tracking detectors.
- Mass of the dissociated photon system in the range $4 < M_{X\ rec} < 32$ GeV. The lower limit eliminates the region dominated by resonance production; it also reflects the lower limit of $M_X = 1.7$ GeV for which Monte Carlo events were generated (cf. section 4). The upper limit is a consequence of the limit on x_L (see below), since $M_X^2 \approx W^2(1 - x_L)$.

In addition, the detection of a high momentum proton in the LPS was required [11]:

- One track in the LPS with $x_L > 0.97$ was required. This is used to select diffractive events in which the proton remains intact.

- Protons with reconstructed trajectories closer than 0.5 mm to the wall of the beam-pipe, at any point between the vertex and the last station hit, were rejected. This eliminates any sensitivity of the acceptance to possible misalignments of the HERA beam-pipe elements. In addition badly reconstructed tracks are removed.
- The p_T range was restricted to the interval $0.27 < p_T < 0.63$ GeV, thereby removing regions where the acceptance of the LPS is very small or changes rapidly [11].

After these selections, 641 events remained.

3.4 Background

The background contamination in the sample was mainly due to two sources.

1. Some activity in the RCAL can accidentally overlap with the scattered positron of a bremsstrahlung event ($ep \rightarrow e\gamma p$) in the LUMI- e [3]. A large fraction of this background can be identified since the bremsstrahlung photon is accepted by the LUMI- γ . For bremsstrahlung, one has $E'_e + E_\gamma = E_e$, where E_γ is the energy of the radiated photon. For such events the energy deposits in the LUMI- e and the LUMI- γ calorimeters thus sum up to the positron beam energy. These events were removed.

The unidentified events were statistically subtracted by including the identified background events with negative weights in all the distributions, thereby compensating for the unidentified background events [26, 27]. This subtraction was less than 3%.

2. A proton beam-halo track in the LPS can accidentally overlap with an event satisfying the trigger and the selection cuts applied to the variables measured with the central ZEUS detector (beam-halo event). The term beam-halo track refers to a proton with energy close to that of the beam originating from an interaction of a beam proton with the residual gas in the pipe or with the beam collimator jaws. Obviously, a beam-halo track is uncorrelated with the activity in the central ZEUS detector. For such a beam-halo event, energy and momentum conservation are not necessarily satisfied; in particular the quantity $(E + P_Z + 2P_Z^{LPS})$, where P_Z^{LPS} is the Z component of the proton momentum measured in the LPS, may exceed the kinematic limit of 1640 GeV. The condition $(E + P_Z + 2P_Z^{LPS}) > 1655$ GeV (thereby including the effects of resolution) identifies such events, which thus were rejected.

In order to evaluate the residual contamination after all cuts, the distribution of $2P_Z^{LPS}$ for identified beam-halo events was randomly mixed with the $(E + P_Z)$ distribution for all events, so as to create a distribution of $(E + P_Z + 2P_Z^{LPS})$ for halo events. The observed $(E + P_Z + 2P_Z^{LPS})$ distribution was then fitted as the sum of the diffractive Monte Carlo contribution (cf. section 4) and the beam-halo contribution just discussed. The relative normalisation of the two terms was left as a free parameter. For events with $(E + P_Z + 2P_Z^{LPS}) < 1655$ GeV, the fraction of beam-halo events thus was estimated to be $(6.3 \pm 1.2)\%$. Here again the identified background events were included with negative weights in all the distributions in order to compensate for the unidentified beam-halo events.

The number of events remaining after the background subtraction, i.e. after removing the identified bremsstrahlung and beam-halo events and after including the effect of the negative weights, was 515. The contribution from non-single diffractive dissociation processes, e.g. double diffractive dissociation, is expected to be of the order of a few per cent [8] and was not subtracted.

Figure 1 shows the observed W , M_X , x_L and p_T distributions for the selected events after background subtraction and including the correction for the effects of the trigger prescale factors.

4 Monte Carlo simulation and acceptance determination

The reaction $ep \rightarrow eXp$ was simulated using a Monte Carlo generator [28] based on a model calculation by Nikolaev and Zakharov [29]. The generated M_X distribution was reweighted with the sum of a pomeron-pomeron-pomeron [7] contribution ($d\sigma/dM_X^2 \propto 1/M_X^2$) and a pomeron-pomeron-reggeon [7] contribution ($d\sigma/dM_X^2 \propto 1/M_X^3$), so as to obtain a satisfactory agreement between data and Monte Carlo. As discussed in sect. 5, however, the present results on the t distribution are largely independent of the details of the M_X spectrum simulation in the mass range considered in the analysis.

All generated events were passed through the standard ZEUS detector simulation, based on the GEANT program [30], and through the trigger simulation package. The simulation also includes the geometry of the beam-pipe apertures, the HERA magnets and their fields. The spread of the interaction vertex position was also simulated and so were the proton beam angle with respect to the nominal direction and its dispersion at the interaction point. The simulated events were then passed through the same reconstruction and analysis programs as the data. In Fig. 1 the distributions for the reconstructed Monte Carlo events as a function of W , M_X , x_L and p_T are compared with those of the data. The distributions of the simulated events were normalised to the observed number of events, corrected for the effects of the prescale and of the background subtraction. The agreement between the data and the Monte Carlo distributions is satisfactory.

The acceptance was computed as the ratio of the number of reconstructed Monte Carlo events in a bin of a given variable and the number of generated events in that bin. The acceptance thus includes the effects of the geometric acceptance of the apparatus, its efficiency and resolution, as well as the trigger and reconstruction efficiencies.

5 Results and discussion

The acceptance corrected t distribution, $dN/d|t|$, is shown in Fig. 2. It was obtained by correcting the measured $t_{apparent}$ distribution bin by bin with the acceptance determined from the Monte Carlo simulation described above.

The data were fitted with the function:

$$\frac{dN}{d|t|} = A \cdot e^{-b|t|}, \quad (3)$$

where A is a constant. The resulting value of the t -slope is

$$b = 6.8 \pm 0.9 \text{ (stat.)}_{-1.1}^{+1.2} \text{ (syst.) GeV}^{-2},$$

in the kinematic region $4 < M_X < 32$ GeV, $0.073 < |t| < 0.40$ GeV² and $176 < W < 225$ GeV. In this region, the average value of W is 200 GeV and the average value of M_X is 11 GeV. The result of the fit is indicated by the continuous line on Fig. 2.

The analysis was repeated for the two M_X ranges $4 < M_X < 8$ GeV and $8 < M_X < 32$ GeV. The results, $b = 7.0 \pm 1.3$ GeV⁻² and $b = 6.5 \pm 1.3$ GeV⁻², indicate no variation with M_X within the present sensitivity.

The quoted systematic uncertainty on b (Δb) was obtained by modifying the requirements and the analysis procedures as listed below:

1. Sensitivity to the selection of the proton track (cf. [11]):

- The sensitivity to the proton beam tilt with respect to the nominal was evaluated by systematically shifting p_T by 10 MeV.
- The track selection requirements were tightened.
- Events with $p_X^{LPS} > 0$ and with $p_X^{LPS} < 0$ were analysed separately, as a check of possible relative rotations of the LPS detector stations.
- The data were divided into a “low acceptance” and a “large acceptance” sample depending on the position of the LPS stations. The latter varied slightly from run to run.

The last three contributions dominate; by summing all four in quadrature, $\Delta b = \pm 1.0$ GeV⁻² was obtained.

2. Sensitivity to the other selection cuts and acceptance corrections:

- The W range was restricted to $195 < W < 215$ GeV, leading to $b = 6.7 \pm 1.4$ GeV⁻².
- The M_X distribution in the Monte Carlo was varied between $d\sigma/dM_X^2 \propto (1/M_X)^{1.5}$ and $d\sigma/dM_X^2 \propto (1/M_X)^3$. The corresponding variation of b was at most ± 0.2 GeV⁻².
- The vertex requirement was removed or restricted to $|Z_{vertex}| < 50$ cm. The effect on b was at most ± 0.4 GeV⁻².

Summing these contributions to Δb in quadrature yields $\Delta b = \pm 0.5$ GeV⁻².

3. Background corrections: the size of the beam-halo background was varied by two standard deviations, yielding negligible effects. The bremsstrahlung background correction was removed altogether, causing changes in the result smaller than 0.1 GeV⁻².

4. Evaluation of the t -slope:

- The t -slope was determined with an alternative method discussed in detail in refs. [11, 31]. One can express the t_{apparent} distribution as a convolution of equation (3) and a two-dimensional Gaussian distribution representing the beam transverse momentum distribution. The slope parameter b can then be determined by fitting the convolution of eq. (3) and the two-dimensional Gaussian to the acceptance corrected t_{apparent} distribution. This method has the advantage that the data can be binned in t_{apparent} for which the resolution is much better than for t , as discussed earlier. The value of b thus obtained was $b = 7.3 \pm 0.9 \text{ GeV}^{-2}$.
- The t -slope was also obtained with a third method: the t_{apparent} distributions in the data and in the Monte Carlo were compared and the Monte Carlo t distribution at the generator level was reweighted until the χ^2 of the comparison between data and Monte Carlo reached a minimum. The result thus found differed from the nominal one by less than 0.1 GeV^{-2} .
- The sensitivity to the binning in t was studied by using an unbinned maximum likelihood method for the fit, which gave a result differing from the nominal one by less than 0.1 GeV^2 .

The quadratic sum of these effects contributes $\Delta b = {}^{+0.5}_{-0.1} \text{ GeV}^{-2}$.

All contributions were summed in quadrature, yielding a total systematic error $\Delta b = {}^{+1.2}_{-1.1} \text{ GeV}^{-2}$.

Table 1 lists the present result together with those of the Fermilab photoproduction experiment E612 [1] and that obtained by ZEUS for $\langle Q^2 \rangle = 8 \text{ GeV}^2$ [8]. The present result agrees within errors with both. This agreement suggests that at fixed W there is little dependence of the slope on Q^2 and that for real photons the W dependence is not strong. Note that the t range of our measurement is different from that of [1], which is $0.02 < |t| < 0.1 \text{ GeV}^2$. A direct comparison should therefore be made with caution: for example, in elastic πp scattering [32], the t -slope measured in the range $0.1 \lesssim |t| \lesssim 0.4 \text{ GeV}^2$ is about 1.2 GeV^{-2} lower than in the range covered by [1]; this difference is of the same size as the errors of our measurement.

The weak Q^2 dependence of the t -slope in diffractive photon dissociation may be contrasted with the change with Q^2 observed for elastic ρ^0 meson production [9-13], where b decreases by approximately $3\text{-}5 \text{ GeV}^{-2}$ when going from $Q^2 \approx 0$ to $Q^2 \approx 10 \text{ GeV}^2$. If factorisation of the diffractive vertices [32] is assumed, the amplitudes for the reactions $\gamma p \rightarrow X p$ and $\gamma p \rightarrow \rho^0 p$ are proportional to the products of vertex functions $G_{\gamma X}(Q^2, t) \cdot G_{pp}(t)$ and $G_{\gamma \rho^0}(Q^2, t) \cdot G_{pp}(t)$, respectively. In this framework, the t -slope includes the sum of the contributions from the γ - X or γ - ρ^0 vertex and from the p - p vertex. The comparison of the $\gamma p \rightarrow X p$ and $\gamma p \rightarrow \rho^0 p$ slopes indicates that the vertex function $G_{\gamma X}(Q^2, t)$ has a weaker dependence on Q^2 than $G_{\gamma \rho^0}(Q^2, t)$. A rapid Q^2 dependence of $G_{\gamma \rho^0}(Q^2, t)$ is expected in pQCD inspired models of elastic vector meson production [33], reflecting the decrease with Q^2 of the transverse size of the quark-antiquark pair into which the photon fluctuates before interacting with the proton. A weak Q^2 dependence of the function $G_{\gamma X}(Q^2, t)$ is also expected in the framework of various models of diffractive dissociation of photons [34].

Acknowledgements

We thank the DESY Directorate for their strong support and encouragement, and the HERA machine group for their diligent efforts. Collaboration with the HERA group was particularly

	Present result	Ref. [1]	Ref. [8]
$\langle Q^2 \rangle / \text{GeV}^2$	≈ 0	0	8
W range/GeV	176-225	12-17	50-270
M_X range/GeV	4-32	1.4-1.7, 1.7-2.2, 2.2-3	2-27
$ t $ range/GeV ²	0.073-0.4	0.02-0.1	0.073-0.4
b/GeV^{-2}	6.8 ± 0.9 (stat.) $^{+1.2}_{-1.1}$ (syst.)	$4.2 \pm 1.4, 6.3 \pm 1.3, 5.1 \pm 1.3$	7.2 ± 1.1 (stat.) $^{+0.7}_{-0.9}$ (syst.)

Table 1: A compilation of results for the t -slope for the reaction $\gamma p \rightarrow Xp$. The present result is listed together with those from ref. [1] for real photons and that of ref. [8] for virtual photons.

crucial to the successful installation and operation of the LPS. We are also grateful for the support of the DESY computing and network services. The design, construction, and installation of the ZEUS detector have been made possible by the ingenuity and dedicated effort of many people from DESY and the home institutes who are not listed as authors; among them we would like to thank B. Hubbard for his invaluable contributions to the experiment, and the LPS in particular. Finally, it is a pleasure to thank N.N. Nikolaev, M.G. Ryskin and M. Strikman for many useful discussions.

References

- [1] E612 Collab., T.J. Chapin et al., Phys. Rev. **D31** (1985) 17.
- [2] H1 Collab., C. Adloff et al., Z. Phys. **C74** (1997) 221.
- [3] ZEUS Collab., J. Breitweg et al., Z. Phys. **C75** (1997) 421.
- [4] J.J. Sakurai, Ann. Phys. **11** (1960) 1.
- [5] T.H. Bauer et al., Rev. Mod. Phys. **50** (1978) 261.
- [6] T. Regge, Nuovo Cimento **14** (1959) 951;
T. Regge, Nuovo Cimento **18** (1960) 947;
see also e.g. P.D.B. Collins, “An Introduction to Regge Theory and High Energy Physics”,
Cambridge University Press, Cambridge (1977).
- [7] R.D. Field and G.C. Fox, Nucl. Phys. **B80** (1974) 367.
- [8] ZEUS Collab., J. Breitweg et al., DESY Report DESY 97-184, to appear in Z. Phys.
- [9] ZEUS Collab., M. Derrick et al., Z. Phys. **C69** (1995) 39.
- [10] H1 Collab., S. Aid et al., Nucl. Phys. **B463** (1996) 3.
- [11] ZEUS Collab., M. Derrick et al., Z. Phys. **C73** (1997) 253.
- [12] ZEUS Collab., M. Derrick et al., Phys. Lett. **B356** (1995) 601.
- [13] H1 Collab., S. Aid et al., Nucl. Phys. **B468** (1996) 3.

- [14] ZEUS Collab., M. Derrick et al., *Z. Phys.* **C73** (1996) 73.
- [15] ZEUS Collab., M. Derrick et al., *Phys. Lett.* **B377** (1996) 259.
- [16] H1 Collab., C. Adloff et al., *Z. Phys.* **C75** (1997) 607.
- [17] H1 Collab., S. Aid et al., *Nucl. Phys.* **B472** (1996) 3.
- [18] ZEUS Collab., J. Breitweg et al., *Z. Phys.* **C75** (1997) 215.
- [19] ZEUS Collab., M. Derrick et al., *The ZEUS Detector, Status Report 1993*, DESY (1993).
- [20] ZEUS Collab., M. Derrick et al., *Phys. Lett.* **B293** (1992) 465.
- [21] C. Alvisi et al., *Nucl. Instr. Meth.* **A305** (1991) 30.
- [22] N. Harnew et al., *Nucl. Instr. Meth.* **A279** (1989) 290;
B. Foster et al., *Nucl. Phys. (Proc. Suppl.)* **B32** (1993) 181;
B. Foster et al., *Nucl. Instr. Meth.* **A338** (1994) 254.
- [23] M. Derrick et al., *Nucl. Instr. Meth.* **A309** (1991) 77;
A. Andresen et al., *Nucl. Instr. Meth.* **A309** (1991) 101;
A. Bernstein et al., *Nucl. Instr. Meth.* **A336** (1993) 23;
A. Caldwell et al., *Nucl. Instr. Meth.* **A321** (1992) 356.
- [24] D. Kisielewska et al., *DESY-HERA Report 85-25* (1985);
J. Andrusków et al., *DESY report DESY 92-066* (1992);
K. Piotrkowski, Ph.D. Thesis, Cracow INP-Exp., *DESY Internal Report F35D-93-06* (1993).
- [25] M. Kasprzak, Ph.D. thesis, Warsaw University, *DESY Internal Report F35D-96-16* (1996).
- [26] ZEUS Collab., M. Derrick et al., *Z. Phys.* **C63** (1994) 391.
- [27] B.D. Burow, Ph.D. Thesis, University of Toronto, *DESY Internal Report F35D-94-01* (1994).
- [28] P. Bruni et al., *Proc. Workshop on Physics at HERA*, DESY, Eds. W. Buchmüller and G. Ingelman (1991) 363;
A. Solano, *Tesi di Dottorato*, University of Torino (1993), unpublished (in Italian).
- [29] N.N. Nikolaev and B.G. Zakharov, *Z. Phys.* **C53** (1992) 331.
- [30] GEANT 3.13, R. Brun et al., *CERN DD/EE/84-1* (1987).
- [31] R. Sacchi, *Tesi di Dottorato*, University of Torino (1996), unpublished (in Italian).
- [32] See e.g.:
G. Alberi and G. Goggi, *Phys. Rep.* **74** (1981) 1;
K. Goulios, *Phys. Rep.* **101** (1983) 169;
M. Kamran, *Phys. Rep.* **108** (1984) 275;
N.P. Zotov and V.A. Tsarev, *Sov. Phys. Uspekhi* **31** (1988) 119;
G. Giacomelli, *Int. J. Mod. Phys. A*, vol. 5, no. 2 (1990), 223.

- [33] See e.g.:
W. Koepf et al., in Proceedings of the “Workshop on Future Physics at HERA”, Hamburg, Sept. 1995-May 1996, Editors G. Ingelman, A. De Roeck, R. Klanner, p. 674, and references therein;
ibid. H. Abramowicz et al., p. 679, and references therein.
- [34] See e.g.:
H. Abramowicz et al., in Proceedings of the “22nd Annual SLAC Summer Institute on Particle Physics”, Stanford, California, 8-19 Aug. 1994, Editors L. De Porcel and J. Chan, SLAC, 1996, p. 539, DESY Report DESY 95-047, and M. Strikman, private communication;
M.G. Ryskin, J. Phys. **G22** (1996) 741, and private communication;
N.N. Nikolaev and B.G. Zakharov, preprint hep-ph/9706343 v2, and Proceedings of the “Fifth International Workshop on Deep Inelastic Scattering and QCD”, Chicago, April 14-18, 1997, Editors D. Krakauer and J. Repond, American Institute of Physics Conference Proceedings no. 407, p. 445, and references therein.

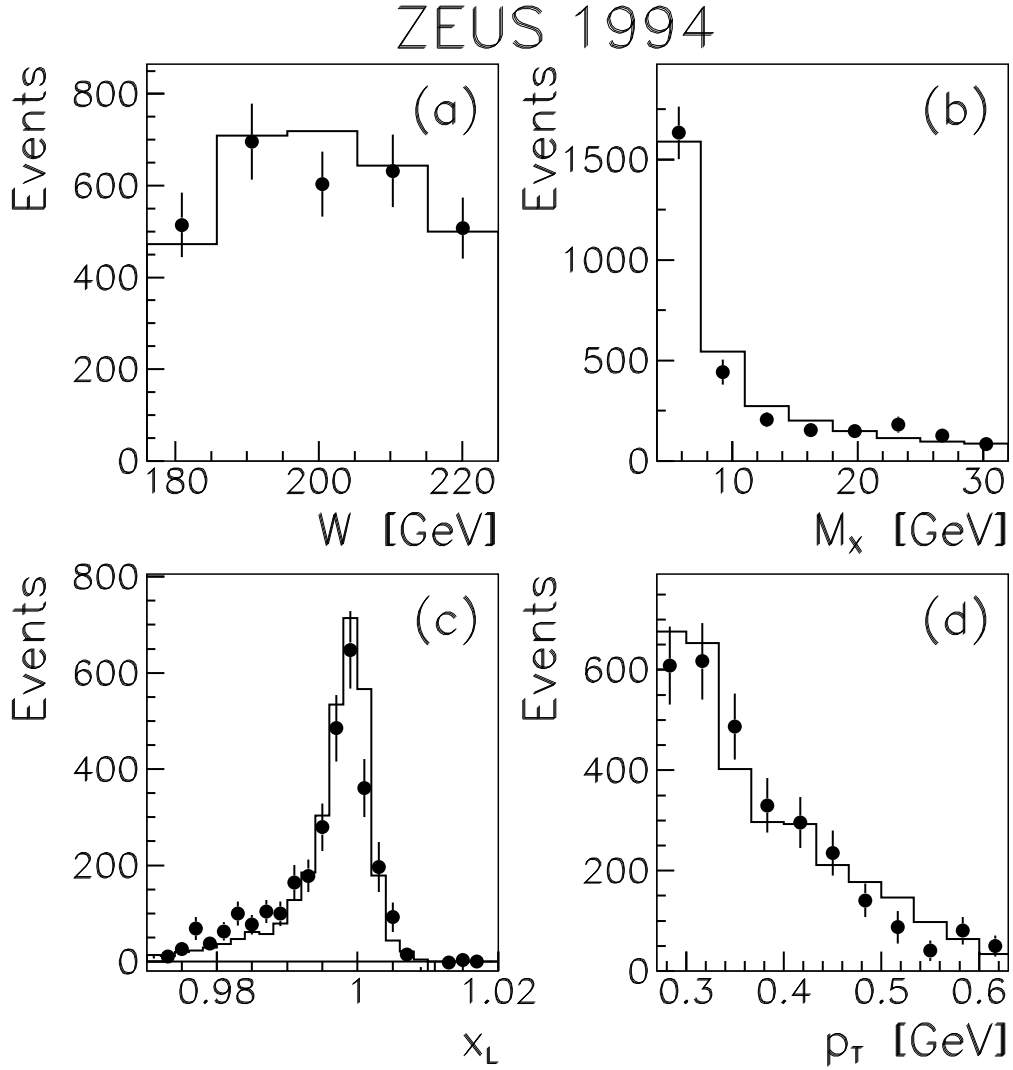


Figure 1: Distributions as a function of (a) W , (b) M_X , (c) x_L and (d) p_T for the data (points) and the Monte Carlo events (histogram). The error bars indicate the statistical uncertainty of the data. The number of data events is corrected for the trigger prescale factors and the background.

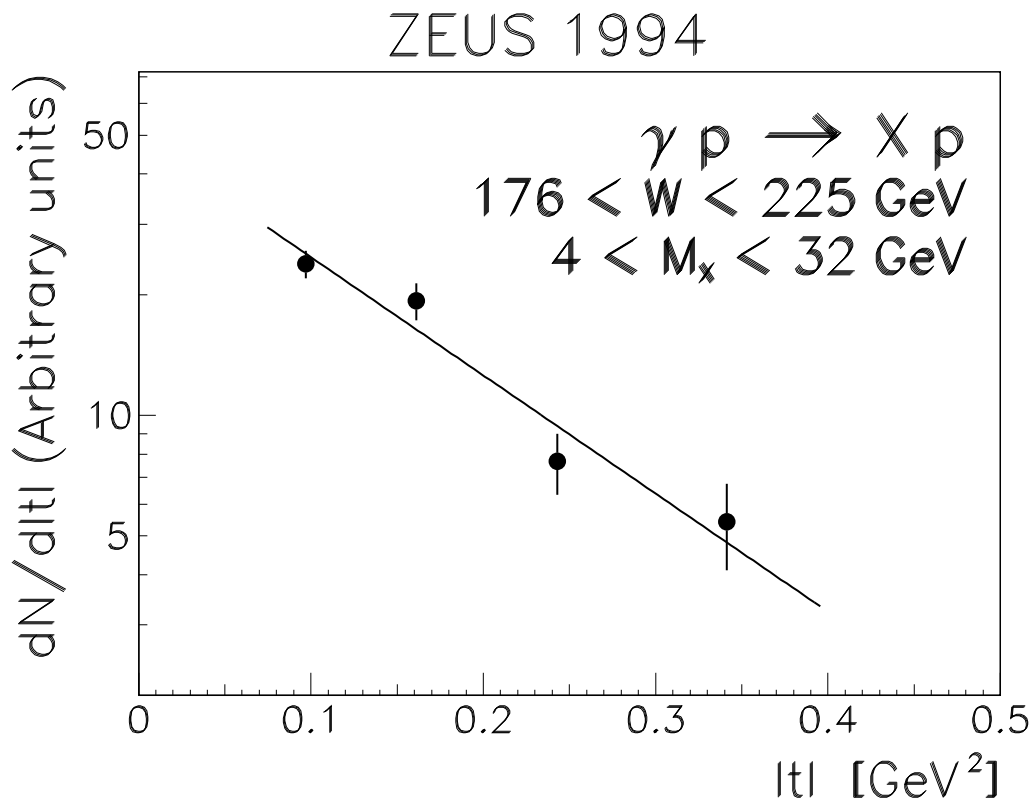


Figure 2: Differential distribution $dN/d|t|$ for photon diffractive dissociation, $\gamma p \rightarrow Xp$, in the kinematic region $176 < W < 225 \text{ GeV}$ and $4 < M_X < 32 \text{ GeV}$. The vertical bars indicate the size of the statistical uncertainties. The line is the result of the fit described in the text. The scale on the vertical axis is arbitrary.